



# Methyltransferase Setd2 prevents T cell–mediated autoimmune diseases via phospholipid remodeling

Yali Chen<sup>ab</sup>, Kun Chen<sup>ac</sup>, Ha Zhu<sup>b</sup>, Hua Qin<sup>d</sup>, Juan Liu<sup>b,1</sup>, and Xuetao Cao<sup>ab,d,1</sup>

Edited by Tak Mak, University of Toronto, Toronto, ON, Canada; received August 23, 2023; accepted December 16, 2023

Coordinated metabolic reprogramming and epigenetic remodeling are critical for modulating T cell function and differentiation. However, how the epigenetic modification controls Th17/Treg cell balance via metabolic reprogramming remains obscure. Here, we find that Setd2, a histone H3K36 trimethyltransferase, suppresses Th17 development but promotes iTreg cell polarization via phospholipid remodeling. Mechanistically, Setd2 up-regulates transcriptional expression of lysophosphatidylcholine acyltransferase 4 (*Lpcat4*) via directly catalyzing H3K36me3 of *Lpcat4* gene promoter in T cells. *Lpcat4*-mediated phosphatidylcholine PC(16:0,18:2) generation in turn limits endoplasmic reticulum stress and oxidative stress. These changes decrease HIF-1 $\alpha$  transcriptional activity and thus suppress Th17 but enhance Treg development. Consistent with this regulatory paradigm, T cell deficiency of *Setd2* aggravates neuroinflammation and demyelination in experimental autoimmune encephalomyelitis due to imbalanced Th17/Treg cell differentiation. Overall, our data reveal that Setd2 acts as an epigenetic brake for T cell–mediated autoimmunity through phospholipid remodeling, suggesting potential targets for treating neuroinflammatory diseases.

Setd2 | lysophosphatidylcholine acyltransferase 4 | phosphatidylcholine | autoimmunity

Pathological autoimmunity is regulated by complex interactions among epigenetic, metabolic, and immune factors (1, 2). T cell dysfunction is a crucial mediator of autoimmune pathogenesis, promoting neuroinflammatory disorders such as multiple sclerosis (MS) (3, 4). Cross-talk between epigenetic and metabolic programs has emerged as a theme in the regulation of T cell fate and function in different pathophysiological conditions (5–8). However, the specific mechanisms by which epigenetic modifiers impact genes encoding metabolic enzymes to determine T cell differentiation remain unknown. Dissecting the interplay between epigenetics and metabolic programs in T cells will foster a better understanding of the pathogenesis underlying autoimmune disease and facilitate the development of disease intervention strategies.

Metabolic networks play variable roles in determining T cell proliferation, activation, differentiation, and survival (5, 8). Effector T cells mainly depend on glycolysis and fatty acid synthesis for differentiation, function, and survival, while Treg cells depend upon oxidative phosphorylation (OXPHOS) and fatty acid oxidation (FAO) (6). Metabolic reprogramming involving glycolysis, glutaminolysis, and lipid synthesis is closely related to T cell dysfunction during autoimmune diseases and tumors (9–12). Lipid metabolism has emerged as a key regulator of T cell fate and function and is closely associated with the pathogenesis of cancer and autoimmunity (8). In particular, phosphatidylcholine (PC) is the most abundant phospholipid in cell membranes and has been linked to inflammatory processes by shaping membrane composition and fluidity (13–15). The lysophosphatidylcholine acyltransferases (LPCATs) are critical for phospholipid remodeling as they catalyze the conversion of lysophosphatidylcholine (LPC) into PC. However, whether reprogramming of LPCAT-mediated phosphatidylcholine metabolism and phospholipid remodeling is linked to T cell polarization and orchestration of Th17/Treg balance remains unknown.

Epigenetic remodeling plays a critical role in immunity and inflammation (16–18). Modulation of chromatin structure and function has emerged as a critical mechanism for coordinating T cell differentiation programs (6, 19). Genes encoding effector cytokines and lineage-determining transcription factors are dynamically controlled by epigenetic mechanisms involving DNA methylation, histone modifications, and non-coding RNAs (20–22). H3K36 methylation is a histone modification linked to active transcription and implicated in immunity and inflammation (23, 24). However, the link between the dynamic reprogramming of H3K36 in Th17/Treg cell differentiation and autoimmune inflammation remains unclear. Setd2 is the only characterized H3K36 trimethyltransferase (H3K36me3) in mammals and has been linked to immunological,

## Significance

Disordered Th17/Treg cell balance in vivo is closely related to the pathogenesis and progression of a variety of autoimmune diseases. In this study, we reveal that the epigenetic modulator Setd2 directly targets the phospholipid remodeling enzyme *Lpcat4* to promote *Lpcat4*-mediated phosphatidylcholine production. Phosphatidylcholine metabolite PC(16:0, 18:2) can limit endoplasmic reticulum stress and suppress HIF-1 $\alpha$  transcriptional activity, thereby alleviating autoimmunity triggered by Th17/Treg cell imbalance. Consistently, in vivo deficiency of Setd2 aggravates the pathological progression of mouse experimental autoimmune encephalomyelitis. Our study reveals a phosphatidylcholine metabolite PC(16:0, 18:2) in controlling Th17/Treg cell balance and provides mechanistic insight into the epigenetic control of metabolic processes in T cell–mediated autoimmunity.

Author contributions: X.C. designed research; Y.C., K.C., and H.Z. performed research; H.Q. contributed new reagents/analytic tools; Y.C. and J.L. analyzed data; and Y.C., J.L., and X.C. wrote the paper.

The authors declare no competing interest.

This article is a PNAS Direct Submission.

Copyright © 2024 the Author(s). Published by PNAS. This article is distributed under Creative Commons Attribution-NonCommercial-NoDerivatives License 4.0 (CC BY-NC-ND).

<sup>1</sup>To whom correspondence may be addressed. Email: juanliu@immunol.org or caoxt@immunol.org.

This article contains supporting information online at <https://www.pnas.org/lookup/suppl/doi:10.1073/pnas.2314561121/-/DCSupplemental>.

Published February 15, 2024.

developmental, and pathological processes including antiviral responses, intestinal epithelial integrity, and embryonic cell development (24–26). So far, the role of *Setd2* in coordinating T cell balance and its link to metabolic regulation remains unclear. Here, we reported a role for *Setd2* in controlling the balance of Th17/Treg cells via phospholipid remodeling, thus adding insights to the interplay between epigenetics and metabolisms in T cell–dependent autoimmunity.

## Results

**Setd2 Expression Is Down-Regulated in T Cell-Mediated Autoimmune Diseases.** In order to test whether H3K36 methylation might be linked to autoimmune disease, we analyzed *SETD2* expression in publicly available sequencing datasets from peripheral blood mononuclear cells isolated from rheumatoid arthritis, skins from psoriasis, and CD4<sup>+</sup> T cells from MS patients (NCBI Gene Expression Omnibus: GSE15573, GSE14905, and GSE16461). We found that *SETD2* expression was down-regulated compared to healthy controls across these autoimmune disease specimens (Fig. 1A). We further validated these results in well-established autoimmune mouse models with experimental autoimmune encephalitis (EAE) and psoriasis. We found that *Setd2* protein and mRNA levels were significantly decreased in CD4<sup>+</sup> T cells from EAE (Fig. 1B and C) and psoriasis mice (Fig. 1D and E). Therefore, *Setd2* gene and protein expression levels are reduced in CD4<sup>+</sup> T cells during the development of a range of autoimmune diseases.

We next used RNA sequencing (RNA-seq) (27) to analyze the expression of 8 reported H3K36 methyltransferases (23) in naive

CD4<sup>+</sup> T, Th0 ( $\alpha$ CD3/CD28), Th17, and induced Treg (iTreg) cells. *Setd2*, *Nsd1*, and *Ash1l* were down-regulated in Th17 and iTreg cells compared with that in naive CD4<sup>+</sup> T cells, while *Smyd2* and *Setd3* expression levels were increased in iTreg cells (Fig. 1F). Compared to that in naive CD4<sup>+</sup> T cells, the *Setd2* mRNA and protein levels in Th17 and iTreg cells were decreased (SI Appendix, Fig. S1). The downregulation of *Setd2* both in CD4<sup>+</sup> T cells from autoimmune diseases and in differentiated Th17 cells indicates a potential correlation between *Setd2* and autoimmune pathogenesis.

**Setd2 Suppresses Th17 and Promotes Treg Differentiation.** The above results inspired us to further investigate the function of *Setd2* in T cell–mediated autoimmunity. To examine the function of *Setd2* in regulating T cells and autoimmunity in vivo, we crossed *Setd2*-*lox* mice (*Setd2*<sup>fl/fl</sup>) (24) with CD4-Cre mice to obtain CD4-specific *Setd2* knockout mice (named as *Setd2*-CD4 cre mice), and the expression of *Setd2* in naive T cells of *Setd2*-CD4 cre mice was significantly lower as compared to the control group (Fig. 2A). We found that *Setd2*-CD4 cre mice had normal populations of lymphocytes and naturally regulated T cells (nTregs) in the thymus (SI Appendix, Fig. S2A). The percentages of T cells, B cells, and CD4<sup>+</sup> and CD8<sup>+</sup> T cells (SI Appendix, Fig. S2B–E) in the spleen and lymph nodes also resembled controls in *Setd2*-CD4 cre mice. These results indicate that the peripheral T lymphocytes of *Setd2*-CD4 cre mice develop normally.

Next, we investigated the changes in T cell proliferation and activation. Notably, the percentages of naive CD4<sup>+</sup> (CD62L<sup>hi</sup>CD44<sup>low</sup>) cells were decreased, and effector/memory CD4<sup>+</sup> (CD62L<sup>low</sup>CD44<sup>hi</sup>) cells were increased in *Setd2*-CD4 cre mice (Fig. 2B), implying

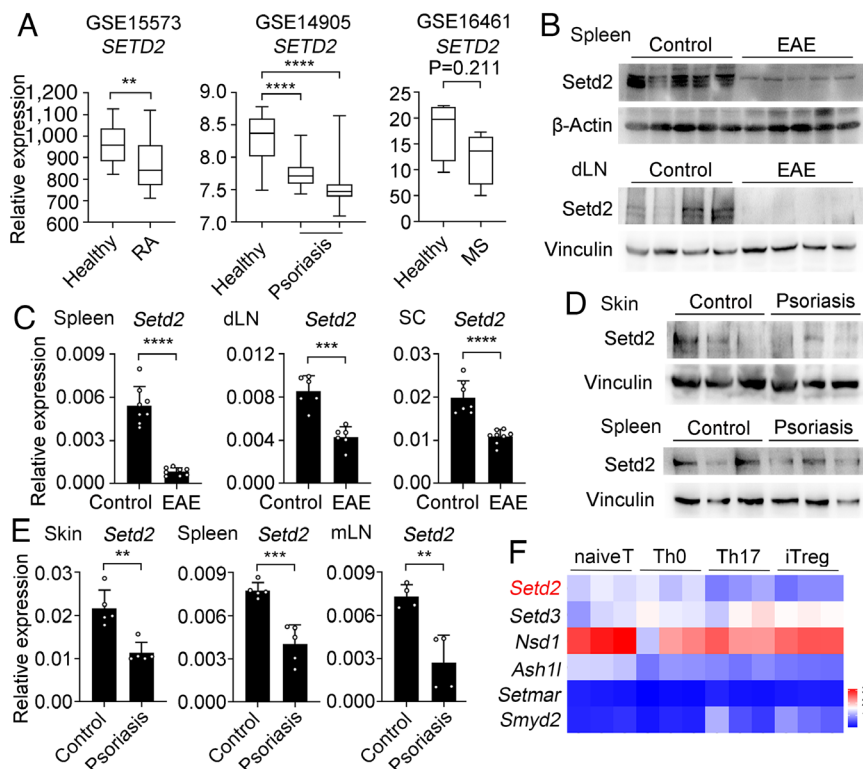


**Fig. 1.** *Setd2* expression is reduced in autoimmune diseases. (A) Boxplot of *SETD2* expression levels in healthy control groups and autoimmune disease groups, rheumatoid arthritis (RA), psoriasis, and multiple sclerosis (MS). (B) Immunoblot analysis of *Setd2* levels of CD4<sup>+</sup> T cells in the spleen and draining lymph node (dLN) from healthy controls and EAE mice. (C) qPCR analysis of *Setd2* mRNA in the spleen, dLN, and spinal cord of EAE specimens and controls (n = 6 to 8). (D) Immunoblot analysis of *Setd2* levels from healthy control and imiquimod induced-psoriasis mice. (E) qPCR analysis of *Setd2* mRNA in the skin, spleen, and mesenteric lymph node (mLN) of healthy controls and psoriasis specimens (n = 4 to 5). (F) The heatmap shows the expression levels of histone H3K36 methyltransferases in naive CD4<sup>+</sup> T, Th0 ( $\alpha$ -CD3/CD28), Th17, and iTreg cells. Data represent one of three independent experiments. Results are presented as means  $\pm$  SD (A, C, and E). \*\**P* < 0.01, \*\*\**P* < 0.001, and \*\*\*\**P* < 0.0001.

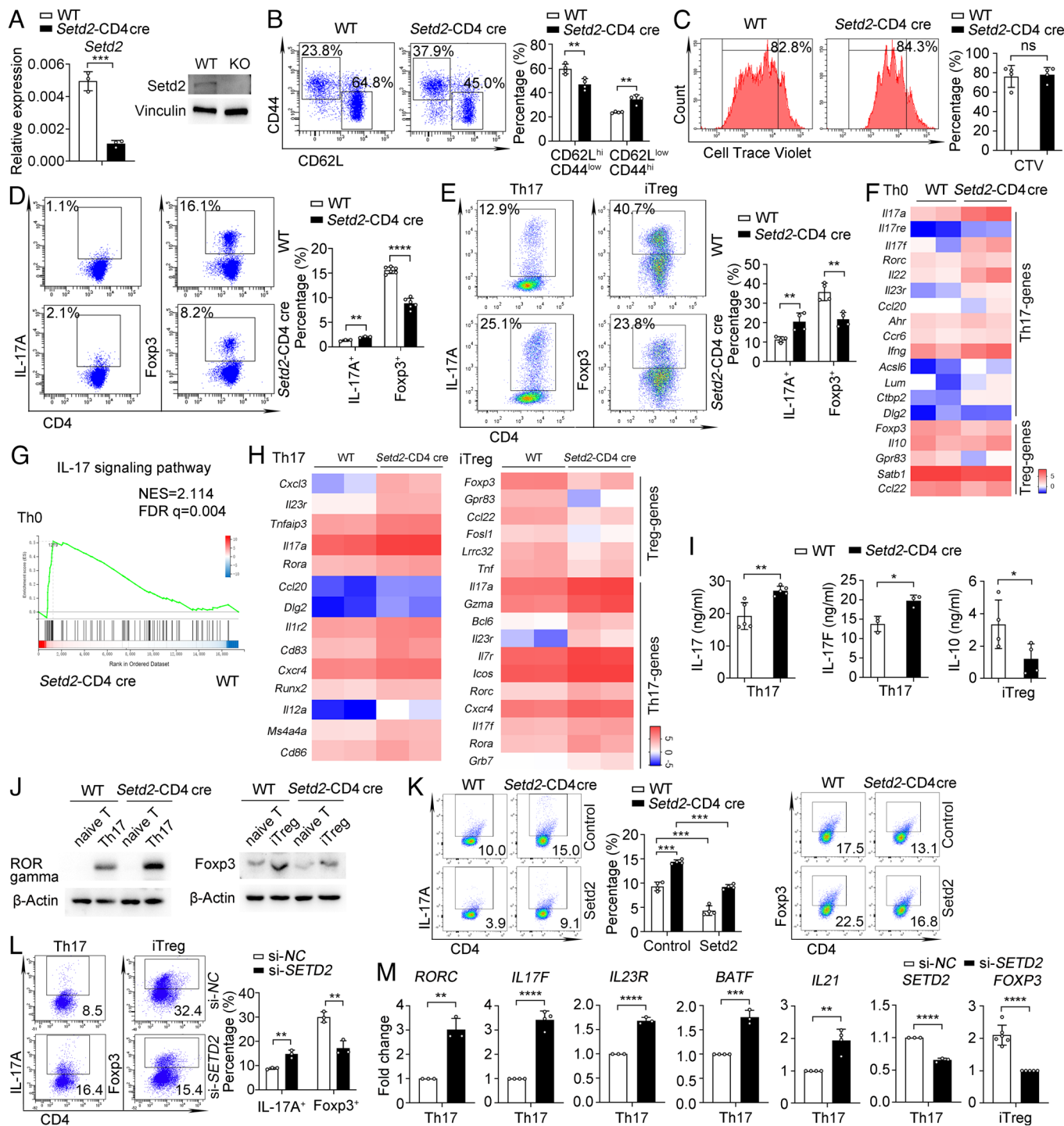


**Fig. 2.** Deletion of *Setd2* promotes Th17 but suppresses Treg cell polarization. (A) mRNA and protein levels of *Setd2* expression in CD4<sup>+</sup> T cells of wild-type (WT) and *Setd2*-CD4 cre mice (n = 3). (B) Flow cytometric analysis of CD62L<sup>+</sup> and CD44<sup>+</sup> cells in splenic CD4<sup>+</sup> T cells from WT and *Setd2*-CD4 cre mice (n = 4). (C) CD4<sup>+</sup> T cell proliferation after treatment with αCD3 (5 μg/mL) and αCD28 (2 μg/mL) for 72 h (n = 4). (D and E) Flow cytometric analysis and quantification of IL-17A<sup>+</sup> and Foxp3<sup>+</sup> cells in splenic CD4<sup>+</sup> T cells (D) and differentiated Th17 and iTreg cells for 3 d (E) (n = 3 to 6). (F) Heatmap shows the differential genes from Th0 cells (fold change > 1.5, P < 0.05). (G) GSEA analysis of enrichment in IL-17 signaling pathway-related genes from Th0 cells. (H) Heatmap showing genes differentially expressed in Th17 cells and iTreg cells (fold change ≥ 2, P < 0.05). (I) CBA analysis of IL-17, IL-17F, and IL-10 in Th17 and iTreg cell supernatants (n = 3 to 5). (J) Immunoblot analysis of RORγt and Foxp3 levels in Th17 and iTreg cells. (K and L) Flow cytometric analysis of IL-17A<sup>+</sup> and Foxp3<sup>+</sup> cells transfected with *Setd2* expressing lentivirus (K) and *SETD2* siRNA (si-*SETD2*) or control siRNA (si-NC) (L) in Th17 and iTreg cells (n = 3 to 4). (M) qPCR analysis of Th17 and Treg-genes expression in human Th17 or iTreg cells transfected with si-*SETD2* or si-NC (n = 3 to 6). Data show one of three independent experiments. Results are presented as means ± SD (A-E, I, and K-M). \*P < 0.05, \*\*P < 0.01, \*\*\*P < 0.001, \*\*\*\*P < 0.0001, and ns, not significant. FDR, false discovery rate. NES, normalized enrichment scores.

that *Setd2*-deficient T cells have increased effector function. However, the proliferation of CD4<sup>+</sup> T cells after treatment with T cell receptor (TCR) was similar in WT and *Setd2*-CD4 cre mice (Fig. 2C).

Based on the above findings, we assessed whether *Setd2* functions in CD4<sup>+</sup> T cell differentiation and function. *Setd2*-deficient mice showed increased IL-17<sup>+</sup> cells and decreased Foxp3<sup>+</sup> cells in their spleens (Fig. 2D). Consistently, *Setd2* deficient CD4<sup>+</sup> T cells

from the spleen (Fig. 2E) and mLN (SI Appendix, Fig. S3A) displayed increased differentiation toward Th17 cells but decreased differentiation toward iTreg cells under in vitro polarization conditions. In addition, *Setd2*-deficient mice showed increased IFN- $\gamma$  cells but unchanged IL-4<sup>+</sup> cells (SI Appendix, Fig. S3 B and C). RNA-seq analysis revealed the upregulation of Th17-related genes, including *Il17a*, *Il17f*, etc. In contrast, the Treg-related genes *Foxp3*, *Il10*, and *Gpr83* were down-regulated in TCR-activated T cells from *Setd2*-deficient mice (Fig. 2F and SI Appendix, Fig. S3 D and E). Gene set enrichment analysis (GSEA) and Kyoto Encyclopedia of Genes and Genomes (KEGG) pathway analysis revealed that the up-regulated genes in *Setd2*-deficient T cells were enriched in IL-17 signaling pathway components (Fig. 2G and SI Appendix, Fig. S3F). These results suggest that *Setd2* plays an important role in inhibiting Th17 but promoting Treg cell differentiation in vitro and in vivo.

We next explored the function of *Setd2* in shaping the gene signatures of polarized Th17 and iTreg cells. RNA-seq showed that signature Th17-related genes were increased and Treg-related signature genes were reduced in *Setd2*-deficient T cells (Fig. 2H and SI Appendix, Fig. S3 G and H). qPCR analysis further verified this phenomenon (SI Appendix, Fig. S3 I and J). In addition, the KEGG pathway analysis identified that the IL-17 signaling pathway and glycerolipid metabolism pathways were enriched in Th17 and iTreg cells (SI Appendix, Fig. S3K). In line with transcript levels, *Setd2*-deficient Th17 cells produced more IL-17 and IL-17F cytokines, while *Setd2*-deficient iTreg cells produced less IL-10 (Fig. 2I). Furthermore, *Setd2* deficiency increased ROR $\gamma$ t and

decreased Foxp3 expression (Fig. 2J). Moreover, overexpression of *Setd2* decreased Th17 and increased iTreg differentiation in both WT and *Setd2*-CD4 cre naive T cells in vitro (Fig. 2K).

Consistent with mouse T cells, silencing of SETD2 in human peripheral blood naive CD4<sup>+</sup> T cells also promoted Th17 differentiation and decreased iTreg differentiation (Fig. 2 L and M and SI Appendix, Fig. S3L). Together, these data demonstrate that *Setd2* specifically inhibits Th17 differentiation and promotes iTreg differentiation.

### Setd2-Mediated H3K36me3 Promotes *Lpcat4* Expression to Mediate Phosphatidylcholine Generation.

To explore the molecular mechanism underlying the imbalance in Th17/Treg cells associated with *Setd2* loss, we further analyzed differentially expressed genes in Th17 cells using transcriptome analysis. RNA-seq analysis revealed that the expression of phosphatidylcholine synthesis-related genes, including *Gpm*, *Lpcat3*, and *Lpcat4*, was decreased in *Setd2*-deficient T cells (Fig. 3A). qPCR confirmed that the expression of phosphatidylcholine synthesis-related genes was down-regulated in *Setd2*-deficient T cells (Fig. 3B and SI Appendix, Fig. S4 A and B), indicating that loss of *Setd2* impairs the phosphatidylcholine synthesis pathway. Phosphatidylcholine is synthesized by two distinct pathways: the de novo and remodeling pathways. Four lysophosphatidylcholine acyltransferase family members, *Lpcat1*, *Lpcat2*, *Lpcat3*, and *Lpcat4* are responsible for catalyzing PC remodeling (13). Intriguingly, the mRNA and protein expression levels of *Lpcat4* were markedly down-regulated

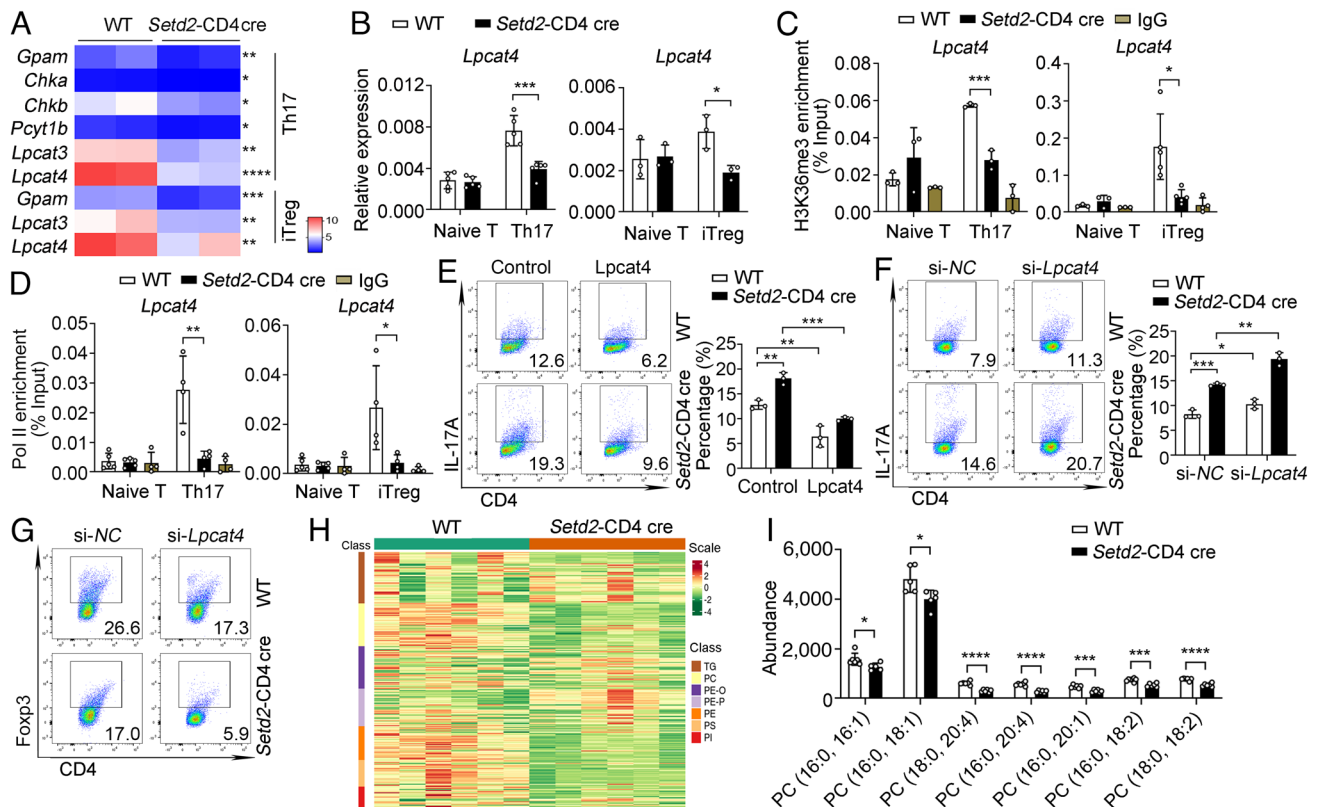


**Fig. 3.** *Setd2*-mediated H3K36me3 promotes *Lpcat4* transcription and phosphatidylcholine generation. (A) Heatmap shows the down-regulated phosphatidylcholine synthesis-related genes in Th17 and iTreg cells (fold change > 1.5,  $P < 0.05$ ). (B) mRNA levels of *Lpcat4* expression in T cells ( $n = 3$  to 5). (C and D) ChIP-qPCR analysis of the enrichment of H3K36me3 (C) or RNA polymerase II (Pol II) (D) at the *Lpcat4* promoter region in T cells ( $n = 3$  to 5). (E) Flow cytometric analysis of IL-17A<sup>+</sup> cells transfected with control and *Lpcat4* expressing lentivirus in Th17 cells ( $n = 3$ ). (F and G) Flow cytometric analysis of IL-17A<sup>+</sup> and Foxp3<sup>+</sup> cells transfected with *Lpcat4* siRNA (si-*Lpcat4*) or control siRNA (si-NC) in Th17 and iTreg cells ( $n = 3$ ). (H) Cluster analysis of lipidomics in Th17 cells from WT and *Setd2*-CD4 cre mice. Six independent samples were analyzed for each group. (I) Lipidomics analysis and quantification of differential phosphatidylcholine species in Th17 cells ( $n = 5$  to 6). Data show one of three independent experiments. Results are presented as means  $\pm$  SD (A-F and I). \* $P < 0.05$ , \*\* $P < 0.01$ , \*\*\* $P < 0.001$ , and \*\*\*\* $P < 0.0001$ .

in *Setd2*-deficient Th17 and iTreg cells (Fig. 3B and *SI Appendix, Fig. S4C*). Thus, *Setd2* up-regulates *Lpcat4* expression in T cells.

*Setd2* trimethylates H3K36, a mark associated with transcriptional activation (23). To test whether *Setd2* controls Th17/Treg cell balance through changes in the *Setd2*-mediated H3K36me3 profile, we measured H3K36me3 levels in T cells. As expected, H3K36me3 levels were increased in Th1, Th17, and iTreg cells (*SI Appendix, Fig. S4D*), suggesting that H3K36me3 is involved in T cell differentiation. Since *Setd2* deficiency significantly reduces *Lpcat4* expression, we wondered whether *Setd2* regulates *Lpcat4* gene expression through its histone methyltransferase activity. ChIP-qPCR results showed that the H3K36me3 modification was enriched at the promoter region of *Lpcat4* in WT cells and was lost in *Setd2*-deficient cells (Fig. 3C). RNA polymerase II (Pol II) can initiate transcription and synthesize mRNA (28). ChIP-qPCR revealed that Pol II occupancy was decreased at the *Lpcat4* promoter region in *Setd2*-deficient T cells (Fig. 3D). Therefore, *Setd2* mediates H3K36me3 modification at the *Lpcat4* gene promoter region, thereby promoting the transcription of the *Lpcat4* gene.

LPCAT family members can catalyze the conversion of LPC to PC and have been linked to both pathological and physiological processes (13). To explore the role of *Lpcat4* in T cell differentiation, we used a pan-lysophospholipid acyltransferase inhibitor, CI-976, that can disrupt the phospholipid remodeling pathway (29). We found that the expression of Th17-related genes was up-regulated and Treg-related genes were down-regulated after CI-976 treatment (*SI Appendix, Fig. S4E*). Furthermore, overexpression of *Lpcat4* significantly down-regulated Th17 and up-regulated iTreg differentiation in both WT and *Setd2*-deficient T cells (Fig. 3E and *SI Appendix, Fig. S4F*). Consistently, silencing of *Lpcat4* also promoted Th17 differentiation and decreased iTreg differentiation (Fig. 3F and G). These data suggest that *Setd2* targets *Lpcat4* to regulate Th17/Treg cell balance and PC remodeling is involved in regulating Th17/Treg cell differentiation.

Next, we performed lipidomics to analyze the lipid composition in Th17 cells. Consistent with transcriptome results, lipidomics analysis revealed that the up-regulated lipid components were significantly enriched in phospholipid biosynthesis and glycerolipid metabolism as analyzed using the Small Molecule Pathway Database (*SI Appendix, Fig. S4G*). Many classes of lipids such as PC, phosphatidylethanolamine (PE), phosphatidylserine (PS), and phosphatidylinositol (PI), were lower in *Setd2*-deficient Th17 cells (Fig. 3H). *Lpcat4* uses acyl CoAs (18:2 or 20:4-acyl-CoA) and oleoyl-CoA (18:1-acyl-CoA) as substrates to form the corresponding PC (13). Our lipidomics data revealed that *Lpcat4*-mediated production of the PC species PC(16:0, 18:1), PC(16:0, 18:2), PC(16:0, 20:4), PC(18:0, 18:2), and PC(18:0, 20:4) was significantly decreased in *Setd2*-deficient Th17 cells (Fig. 3I). Overall, our data indicate that *Setd2* promotes H3K36 trimethylation at the *Lpcat4* promoter, thus increasing *Lpcat4* expression and PC generation.

**Lpcat4-Mediated PC(16:0, 18:2) Generation Controls Th17/Treg Cell Balance.** Next, we tested the proposal that *Setd2*-mediated PC generation is involved in Th17/Treg balance. We measured the effect of stimulating CD4<sup>+</sup> T cells with two commercially available PCs: PC(16:0, 18:1) or PC(16:0, 18:2). PC(16:0, 18:1) treatment did not affect Th17 and iTreg cell polarization or cytokine expression (*SI Appendix, Fig. S5*). These data suggest that PC(16:0, 18:1) does not affect Th17 or iTreg differentiation.

In contrast, the proportion of Th17 cells was decreased and iTreg cells were increased compared to the control group after PC(16:0, 18:2) treatment (Fig. 4A). Consistently, Th17 differentiation markers

were down-regulated and iTreg markers were increased in the presence of PC(16:0, 18:2) (Fig. 4B and C). In addition, the PC(16:0, 18:2)-treated Th17 cells produced less IL-17 and more IL-10 in PC(16:0, 18:2)-treated iTreg cells (Fig. 4D). Thus, PC(16:0, 18:2) can contribute to regulating Th17/Treg cell balance.

We further examined whether PC(16:0, 18:2) is responsible for *Setd2*-mediated T cell differentiation. We found that PC(16:0, 18:2) can reduce the differentiation of *Setd2*-deficient Th17 cells and enhance the differentiation of *Setd2*-deficient iTreg cells (Fig. 4E–G). Collectively, these data demonstrate that *Setd2* promotes *Lpcat4*-mediated PC(16:0, 18:2) generation to control Th17/Treg cell balance.

**Setd2 Promotes PC(16:0, 18:2) Generation to Limit ER Stress and Oxidative Stress.** We next sought to further define the molecular mechanisms underlying PC-mediated control of T cell balance. Distinct PCs have unique acyl-chain composition and membrane remodeling properties that play variable roles in regulating inflammation (30, 31). LPCAT family members were previously shown to regulate tissue PC acyl-chain composition: for example, *Lpcat3* can change the composition of membrane phospholipids and ameliorate endoplasmic reticulum (ER) stress and tissue inflammation (31). We therefore hypothesized that the *Setd2*/PC(16:0, 18:2) axis may regulate ER stress during T cell differentiation. Interestingly, PC(16:0, 18:2) significantly reduced the mRNA expression of ER stress makers and ER stress-related proteins in Th17 and iTreg cells (Fig. 5A and *SI Appendix, Fig. S6A and B*). Cells undergoing ER stress can be identified by increased ER-tracker probe uptake (32). In addition, treatment with PC(16:0, 18:2) was associated with a reduction in ER-tracker mean fluorescence intensity (MFI) in Th17 and iTreg cells (Fig. 5B). These data indicate that *Lpcat4*-mediated synthetic product PC(16:0, 18:2) can restrain ER stress signaling pathway.

The observation that PC(16:0, 18:2) can restrain ER stress and regulate Th17/Treg cell balance, prompted us to test whether *Setd2* feeds into the same pathway and is linked to ER stress-associated T cell differentiation. In our RNA-seq data, several ER stress markers were up-regulated in *Setd2*-deficient T cells (Fig. 5C). These ER stress markers and signaling proteins were also increased in *Setd2*-deficient T cells (Fig. 5D and E). ER stress is generally associated with enlarged ER lumen size in cells that can be detected with an ER tracker probe using confocal microscopy (32). Confocal microscopy imaging showed that the ER lumen was larger in *Setd2*-deficient Th17 cells (Fig. 5F). The data indicate that similar to PC(16:0, 18:2), *Setd2* can inhibit the ER stress response in Th17 and iTreg cells.

Given the comparable role of *Setd2* and PC(16:0, 18:2) in inhibiting ER stress and regulating Th17/Treg differentiation, we speculated that *Setd2* may control Th17/Treg cell balance by promoting PC(16:0, 18:2)-mediated inhibition of ER stress. As expected, PC(16:0, 18:2) could largely reverse the up-regulated ER stress signaling (Fig. 5G) and ER abundance (Fig. 5H and I and *SI Appendix, Fig. S6C*) in *Setd2*-deficient Th17 or iTreg cells. By using 4-phenylbutyric acid (4-PBA), an ER stress inhibitor, we showed that 4-PBA significantly reduced Th17 differentiation in both WT and *Setd2*-CD4 cre T cells (*SI Appendix, Fig. S6D*). Together, these results demonstrate that *Setd2* deficiency suppresses PC(16:0, 18:2) to restrict the ER stress response, thereby controlling Th17/Treg cell balance.

ER stress is accompanied by oxidative stress and reactive oxygen species (ROS) production, which plays an important role in Th17/Treg imbalance-mediated autoimmune diseases (33, 34). Therefore, we investigated whether *Setd2*/PC(16:0, 18:2)-mediated inhibition of ER stress may alter the oxidative stress response of

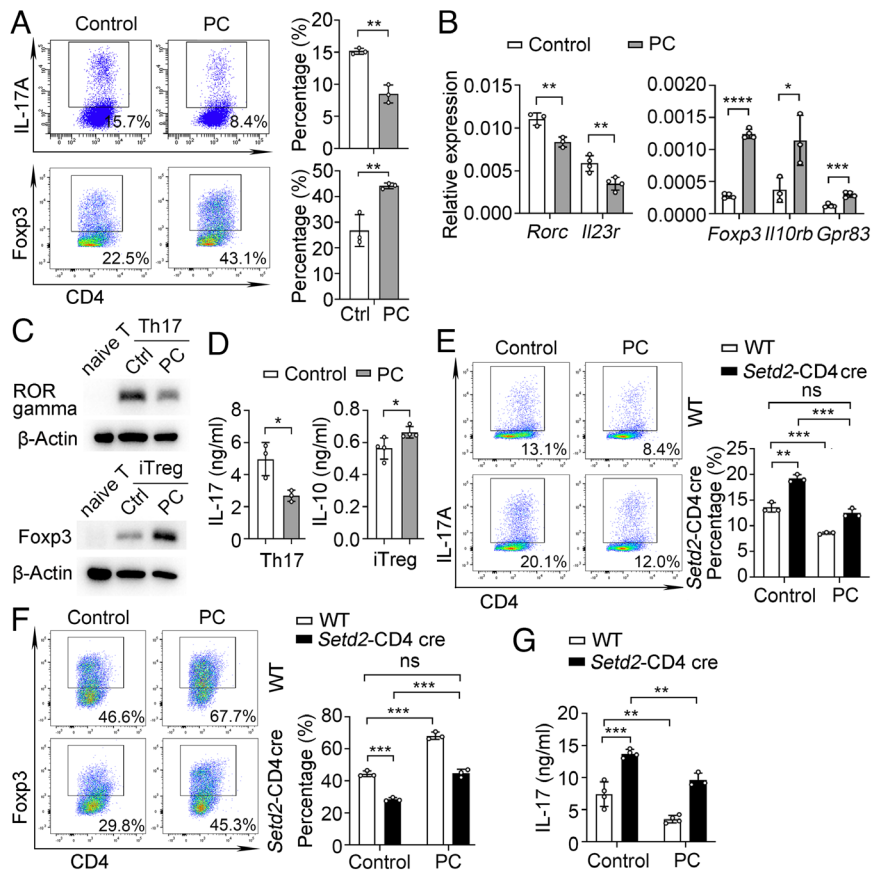


**Fig. 4.** Lpcat4-mediated PC(16:0, 18:2) controls Th17/Treg cell balance. (A) Flow cytometric analysis of IL-17A<sup>+</sup> in Th17 (Top) and Foxp3<sup>+</sup> in iTreg (Below) cells after treatment with solvent control (Ctrl) or PC(16:0, 18:2) (PC, 50 μM) (n = 3). (B) qPCR analysis of *Rorc*, *Il23r*, *Foxp3*, *Il10rb*, and *Gpr83* mRNA expression in Th17 and iTreg cells after stimulation with control or PC (n = 3 to 4). (C) Immunoblot analysis of RORγt and Foxp3 levels in Th17 and iTreg cells after PC and Ctrl treatments. (D) CBA analysis of IL-17 in Th17 and IL-10 in iTreg cells after PC and Ctrl treatment (n = 3 to 4). (E and F) Flow cytometric analysis of IL-17A<sup>+</sup> and Foxp3<sup>+</sup> in Th17 and iTreg cells from WT and *Setd2*-CD4 cre mice (n = 3) after PC or Ctrl treatment. (G) CBA analysis of IL-17 in Th17 cell after PC or Ctrl treatment (n = 3 to 4). Data show one of three independent experiments. Results are presented as means ± SD (A, B, and D–G). \*P < 0.05, \*\*\*P < 0.01, \*\*\*\*P < 0.001, \*\*\*\*\*P < 0.0001, and ns, not significant. PC referred to PC(16:0, 18:2).

Th17/Treg cells. We found that the deletion of *Setd2* promotes the production of ROS in Th17 and iTreg cells, while treatment with 4-PBA significantly reduces the production of ROS in *Setd2*-deficient T cells (Fig. 5 J and K). N-acetyl cysteine (NAC), is a scavenger of ROS (35). ROS is known to function in autophagy and phagocytosis (36–38). We also observed a significant enrichment in the expression of genes linked to phospholipid phagocytosis in *Setd2*-deficient T cells (SI Appendix, Fig. S6E), further supporting a model where *Setd2* inhibits ROS production by regulating phospholipid production. Next, we tested the role of PC in regulating ROS production and found that PC(16:0, 18:2) treatment significantly reduced ROS levels in WT and *Setd2*-deficient T cells (Fig. 5 L and M). Endoplasmic reticulum oxidoreductin 1-alpha (Ero1α) is an enzyme in ROS production. Consistently, PC(16:0, 18:2) also down-regulated the expression of Ero1α in WT and *Setd2*-deficient Th17 cells (SI Appendix, Fig. S6F). These results demonstrate that *Setd2* inhibits ER stress and the subsequent oxidative stress response by promoting PC(16:0, 18:2) generation.

**Setd2 Promotes PC(16:0, 18:2) Generation to Restrict HIF-1α Transcription in T Cells.** HIF-1α is a key transcription factor that controls the balance between Th17 and Treg differentiation (39). ROS is known to be essential for HIF-1α activation by inhibiting the activity of the prolyl hydroxylase domain and enhancing

HIF-1α stability (7, 40). Therefore, we explored whether *Setd2* regulates Th17/Treg cell balance by reducing the oxidative stress response and thus altering the activity of HIF-1α. In RNA-seq data, we found that genes linked to the HIF-1 signaling pathway were up-regulated in *Setd2*-deficient iTreg cells (Fig. 6A). We also detected increased HIF-1α mRNA and protein expression in the *Setd2*-CD4 cre mice (Fig. 6 B and C). ChIP-qPCR revealed that HIF-1α directly binds to the *Rorc* and *Il17* promoter, and *Setd2* deficiency can increase the enrichment of HIF-1α binding to the *Rorc* and *Il17* promoter region (Fig. 6D). These results indicate that *Setd2* can inhibit HIF-1α transcriptional activity to suppress *Rorc* and *Il17* expression.

Moreover, PC(16:0, 18:2) directly inhibits HIF-1α expression in WT Th17 and iTreg cells (Fig. 6 E and F), and ChIP-qPCR results show that PC(16:0, 18:2) can significantly reduce the binding ability of HIF-1α to the *Rorc* and *Il17* promoter region (Fig. 6G). PC(16:0, 18:2) also diminishes *Hif1a* transcript levels in *Setd2*-deficient Th17 cells (Fig. 6H), suggesting that *Setd2* inhibits the transcriptional activity of HIF-1α by promoting Lpcat4-mediated PC(16:0, 18:2) generation.

**Setd2 Deficiency Exacerbates T Cell-Mediated Autoimmunity In Vivo.** We next explored the role of *Setd2* in the development of T cell-mediated autoimmune diseases in a multiple sclerosis mouse model, experimental autoimmune encephalomyelitis. We found

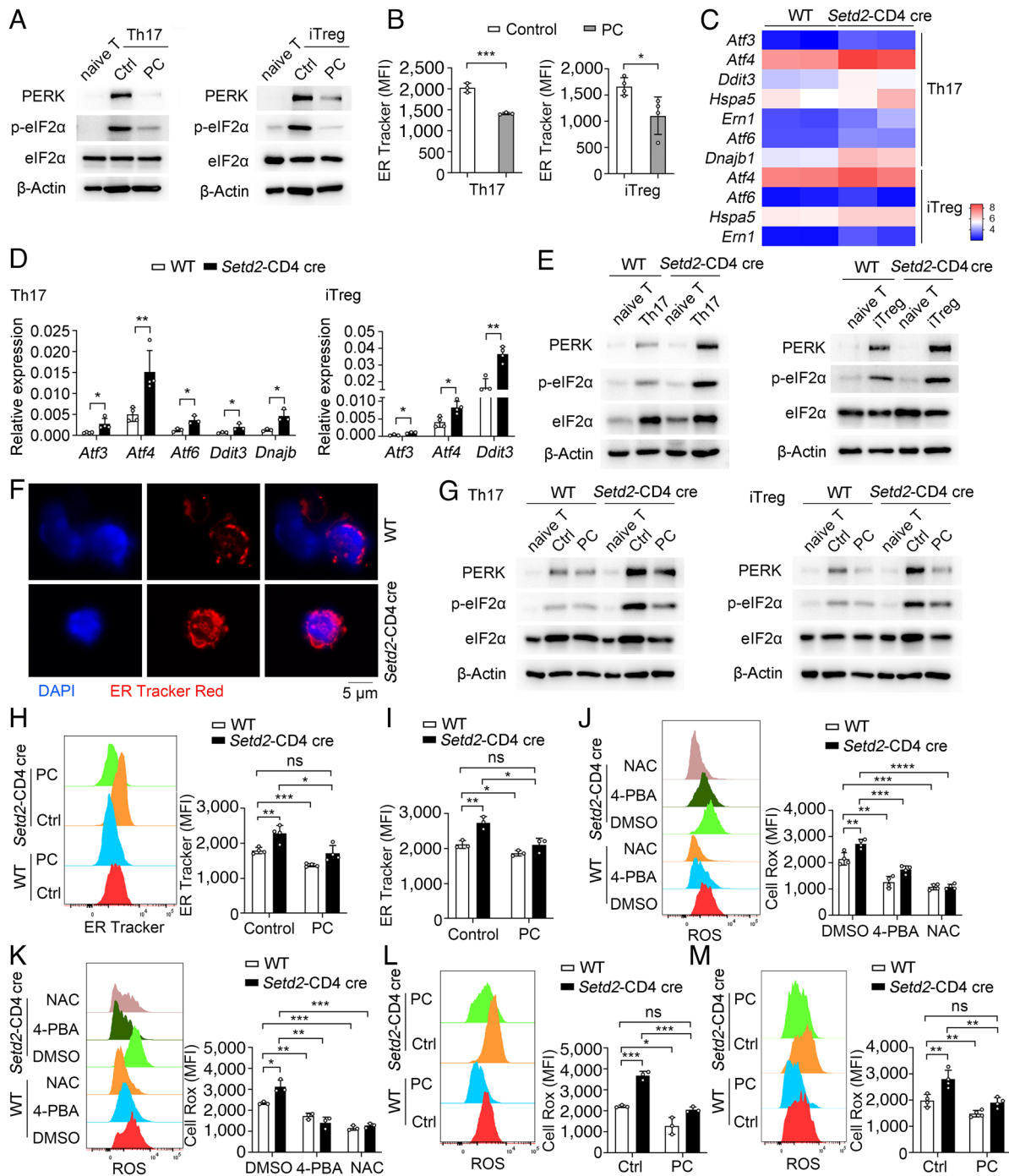


**Fig. 5.** *Setd2* promotes PC(16:0, 18:2) generation to limit ER stress and the oxidative stress response. (A) PERK and phospho-eIF2 $\alpha$  levels in T cells treated with PC(16:0, 18:2) and controls. (B) Flow cytometric analysis of ER tracker mean fluorescence intensity (MFI) in T cells treated with control or PC ( $n = 3$  to 4). (C) Heatmap showing differentially expressed ER stress markers in T cells (fold change  $> 1.5$ ,  $P < 0.05$ ). (D and E) ER stress markers mRNA and protein expression in T cells ( $n = 3$  to 4). (F) Immunofluorescence analysis of ER Tracker Red (red) and DAPI (blue) in Th17 cells. (Scale bar, 5  $\mu\text{m}$ .) (G) The protein levels of PERK and phospho-eIF2 $\alpha$  in WT and *Setd2*-deficient Th17 and iTReg cells stimulated with control or PC. (H and I) Analysis of ER tracker MFI in Th17 (H) and iTReg (I) cells treated with control or PC ( $n = 3$  to 4). (J and K) Flow cytometric analysis of Cell Rox MFI in Th17 (J) and iTReg (K) cells stimulated with DMSO, 4-PBA (1 mM), and NAC (1 mM) ( $n = 3$  to 4). (L and M) Flow cytometric analysis of Cell Rox MFI in Th17 (L) and iTReg (M) cells treated with control or PC(16:0, 18:2) ( $n = 3$  to 4). Data show one of three independent experiments. Results are presented as means  $\pm$  SD (B, D, and H–M). \* $P < 0.05$ , \*\* $P < 0.01$ , \*\*\* $P < 0.001$ , \*\*\*\* $P < 0.0001$ , and ns, not significant.

that *Setd2*-deficient mice showed more severe disease symptoms and had a higher clinical score, peak score, and increased loss of body weight compared to WT mice (Fig. 7 A–C). In addition, *Setd2*-CD4 cre mice showed a significant increase in CD4<sup>+</sup> T and Th17 cell infiltration, while the infiltration of Treg cells was reduced in *Setd2*-CD4 cre mice (Fig. 7 D–F and SI Appendix, Fig. S7A). Consistently, the expression of *Rorc*, *Il17*, *Il17f*, *Batf*,

and *Il22* was markedly increased, whereas *Foxp3*, *Il10*, and *Il10ra* were reduced in the spleen and brain (Fig. 7G and SI Appendix, Fig. S7 B and C). Moreover, in vitro MOG<sub>35-55</sub> peptide recall analysis substantially elevated IL-17 and IFN- $\gamma$  production in *Setd2*-deficient splenocytes (Fig. 7H). Histological analysis showed increased lymphocyte infiltration into the spinal cords of *Setd2*-CD4 cre mice and more severe demyelination (Fig. 7 I–K). These

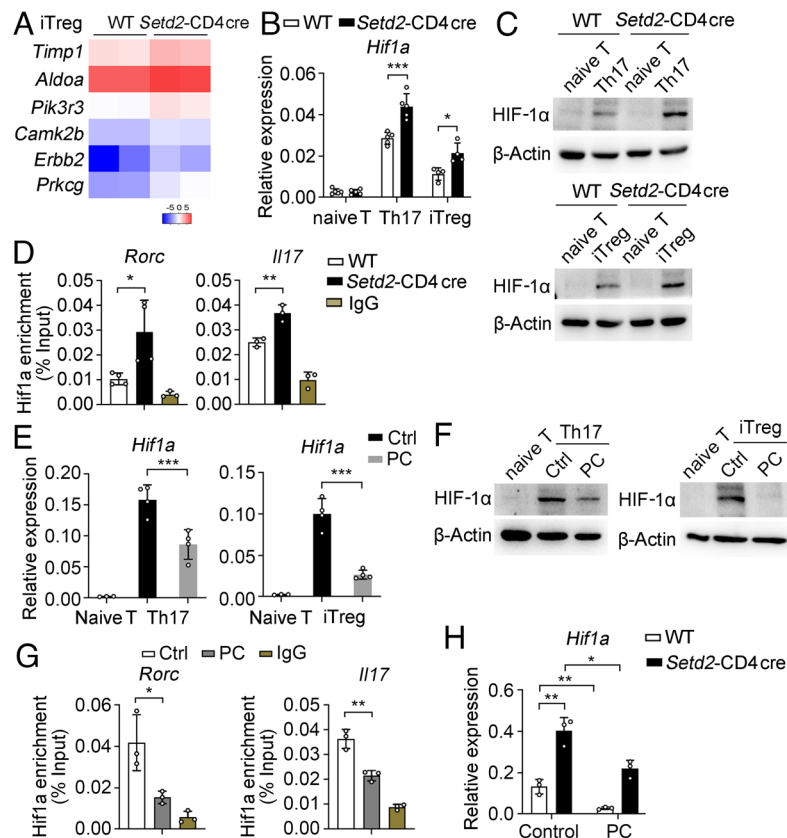


**Fig. 6.** *Setd2* increases PC(16:0, 18:2) levels to inhibit HIF-1 $\alpha$  transcriptional activity. (A) Heatmap showing HIF-1 signaling-linked genes in iTreg cells (fold change  $\geq 2$ ,  $P < 0.05$ ). (B and C) mRNA and protein levels of HIF-1 $\alpha$  in T cells ( $n = 4$  to 5). (D) ChIP-qPCR analysis of HIF-1 $\alpha$  enrichment at the *Rorc* and *I17* promoter region in Th17 cells ( $n = 3$  to 4). (E and F) mRNA and protein levels of HIF-1 $\alpha$  in Th17 and iTreg cells after stimulation with control or PC(16:0, 18:2) ( $n = 3$  to 4). (G) ChIP-qPCR analysis of the enrichment of Hif1 $\alpha$  at the *Rorc* and *I17* promoter regions in Th17 cells after stimulation with control or PC ( $n = 3$ ). (H) qPCR analysis of *Hif1a* mRNA in Th17 cells after stimulation with control or PC ( $n = 3$ ). Data show one of three independent experiments. Results are presented as means  $\pm$  SD (B, D, E, G, and H). \* $P < 0.05$ , \*\* $P < 0.01$ , and \*\*\* $P < 0.001$ .

results demonstrate that CD4<sup>+</sup> T cell-specific deletion of *Setd2* aggravates EAE immunopathology by regulating the balance of Th17/Treg cell differentiation.

To directly examine the cell-intrinsic function of *Setd2* in CD4<sup>+</sup> T cells, we transferred naive CD4<sup>+</sup> T cells from WT and *Setd2*-CD4 cre mice into *Rag2*<sup>-/-</sup> hosts to induce the EAE model. *Rag2*<sup>-/-</sup> hosts that received *Setd2*-deficient CD4<sup>+</sup> T cells showed higher clinical scores and increased loss of body weight (Fig. 7 L and M), and significantly increased CD4<sup>+</sup> T cells and IL-17A<sup>+</sup> cells infiltration and also reduced Foxp3<sup>+</sup> cells (Fig. 7 N and O and SI Appendix, Fig. S7D). In addition, expression of the inflammatory cytokines was significantly increased in recipients of *Setd2*-deficient T cells (Fig. 7 P and Q). Histological analysis showed the infiltration of lymphocytes into the spinal cord was increased along with more severe demyelination in recipients of *Setd2*-deficient T cells (SI Appendix, Fig. S7E). To investigate whether PC(16:0,18:2) has a therapeutic effect on autoimmune diseases in *Setd2*-CD4 cre mice, we used an EAE model in vivo to show that PC(16:0,18:2) treatment significantly reduced Th17 cell infiltration and enhanced the numbers of Treg cell both in WT and *Setd2*-deficient mice, as compared to the control treatment (SI Appendix, Fig. S7 F–I). The data suggest that PC(16:0,18:2) could rescue *Setd2*-CD4 cre mice from the T cell imbalance during autoimmunity, potentially exerting a therapeutic effect on autoimmune diseases. Together, these data demonstrate that *Setd2* deficiency exacerbates CD4<sup>+</sup> T cell-mediated autoimmunity that correlates with Th17/Treg cell imbalance.

## Discussion

Here, we have uncovered a cross-regulatory mechanism that links epigenetic modification and phospholipid metabolism in autoimmunity. Our study reveals a function for *Setd2*-mediated H3K36me3 modification in regulating Th17/Treg cell balance via *Lpcat4*-based phospholipid remodeling. The metabolite PC(16:0, 18:2), produced by *Lpcat4*, can inhibit endoplasmic reticulum stress and the oxidative stress response, thus reducing HIF-1 $\alpha$  transcriptional activity and suppressing Th17 differentiation and promoting Treg differentiation. Our study, therefore, reveals a significant role for the phospholipid PC(16:0, 18:2) in controlling Th17/Treg cell balance and also provides mechanistic insight into the epigenetic control of metabolic processes in T cell-mediated autoimmunity.

H3K36 modifications have been shown to regulate T cell differentiation and function. *Setd2*, as a H3K36 trimethyltransferase, has been studied primarily in tumors and nonimmune cells (24, 26, 41). Although evidence has shown that *Setd2* facilitates ROR $\gamma$ <sup>+</sup> Treg homeostasis in group 3 innate lymphoid (ILC3) cells and suppresses intestinal inflammation (41), the role of *Setd2* in T cell-mediated autoimmune diseases has remained untested. In our study, we found reduced *Setd2* expression in multiple autoimmune diseases, including psoriasis, rheumatoid arthritis, and experimental autoimmune encephalomyelitis. Functionally, *Setd2* prevents autoimmune pathogenesis by suppressing Th17 cell differentiation and promoting Treg cell differentiation through H3K36 trimethylation. Therefore, we suggest *Setd2* acts as an

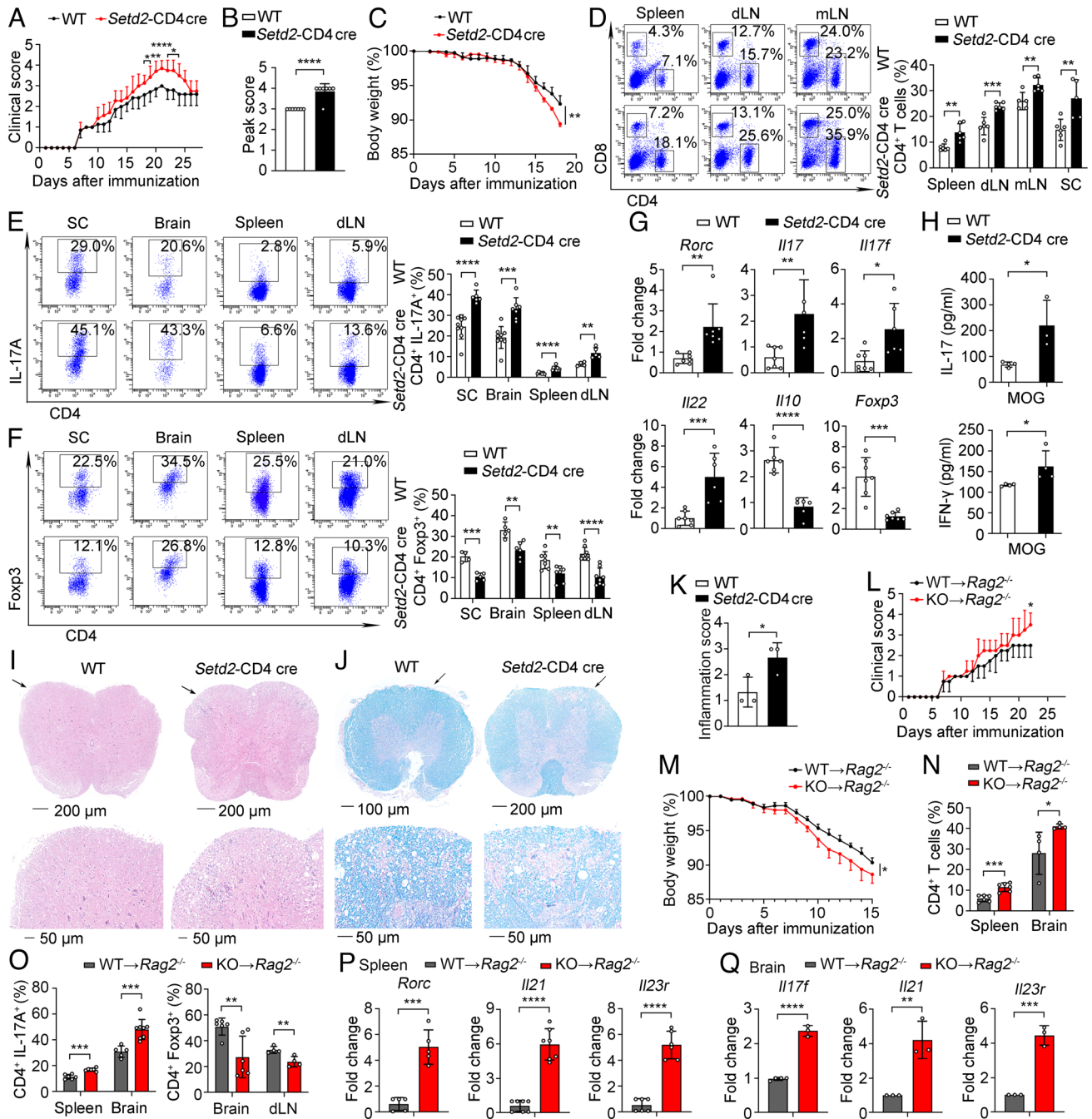


**Fig. 7.** Deficiency of *Setd2* aggravates the severity of the autoimmune disease. (A–C) Clinical scores (A), peak scores (B), and body weight (C) of WT and KO mice after induced EAE (n = 4 to 7). (D) Frequency of CD4<sup>+</sup> and CD8<sup>+</sup> T cells in the spleen, dLN, mLN, and SC (n = 5 to 6). (E and F) Frequency of IL-17A<sup>+</sup> and Foxp3<sup>+</sup> cells in the SC, brain, spleen, and dLN (n = 4 to 9). (G) mRNA expression of inflammatory genes in the spleen (n = 5 to 7). (H) Splenocytes were rechallenged with MOG<sub>35–55</sub> peptide (20 μg/mL) for 3 d; IL-17 and IFN-γ were assessed by CBA (n = 3 to 4). (I and J) Representative histology of the spinal cord stained with hematoxylin and eosin (I) and Luxol fast blue (J) after EAE induction (day 21). (K) Inflammation scores of spinal cords are shown (n = 3). (L–Q) Adoptive transfer of WT and *Setd2*-deficient CD4<sup>+</sup> T cells into *Rag2*<sup>-/-</sup> host mice. (L and M) Clinical scores and body weight of *Rag2*<sup>-/-</sup> host mice after EAE induction (n = 4). (N and O) Quantification of CD4<sup>+</sup>, IL-17A<sup>+</sup>, and Foxp3<sup>+</sup> cells in the spleen, brain, and dLN (n = 4 to 6). (P and Q) mRNA expression of inflammatory genes in the spleen and brain (n = 3 to 7). Data show one of two or three independent experiments. Results are presented as means ± SD (A–H and K–Q). \*P < 0.05, \*\*P < 0.01, \*\*\*P < 0.001, and \*\*\*\*P < 0.0001. KO referred to *Setd2*-CD4 cre mice.

indispensable brake that usually prevents harmful autoreactive T cell responses. Potential strategies for enforcing *Setd2* expression and function may provide opportunities for the treatment of autoimmune and inflammatory diseases.

Dysregulation of lipid metabolism is related to many diseases, including chronic inflammation, autoimmunity, cancer, and metabolic and degenerative diseases (7, 42). The involvement of lipid metabolites as well as their catalyzing enzymes in T cell

differentiation is attracting increasing attention. One recent study showed that lysophosphatidylethanolamine synthase *Pla2g12a* produces 1-Oleoyl-lysophosphatidylethanolamine [LPE (1-18:1)], which can directly bind to RORγt and promote RORγt transcriptional activity (43). Our study revealed a phospholipid remodeling enzyme *Lpcat4* is regulated by an epigenetic mechanism, and *Lpcat4*-mediated metabolite PC(16:0, 18:2) can inhibit the transcriptional activity of HIF-1α to regulate Th17/Treg cell balance.

Therefore, phospholipids play widespread roles in determining Th17 cell generation. As LPE (1-18:1) contained *sn-1* saturated fatty acids but PC(16:0, 18:2) contained *sn-2* unsaturated fatty acid linoleic acid, we suspected that the opposite role of LPE (1-18:1) and PC(16:0, 18:2) was likely due to their differential fatty acyl chain component and property. Whether PC(16:0, 18:2) directly binds to key protein regulators such as HIF1 $\alpha$  and ROR $\gamma$ t in Th17 cells requires further exploration.

LPCAT family members participate in phospholipid remodeling (13). LPCAT1, LPCAT2, and LPCAT3 are mainly involved in the pathogenesis of cancer and hepatocellular inflammation (44, 45). However, little is known about the molecular mechanisms controlling LPCAT expression or the potential immunological functions of this family. Here, we have revealed a role for *Lpcat4* in controlling T cell polarization via PC remodeling. We found that *Setd2* directly targets *Lpcat4* and thereby promotes LPCAT4-dependent unsaturated PC generation. Since PCs are the main component of the cell membrane, it will be interesting to further explore whether *Setd2*-regulated unsaturated PC affects membrane fluidity or membrane microdomains in the regulation of T cell immunity.

Dysregulated ER stress can initiate inflammatory responses and metabolic abnormality, leading to a series of human diseases, including autoimmune and neurodegenerative disorders. However, the endogenous pathways that restrain ER stress to maintain immune homeostasis remained unknown. Here, we report that *Lpcat4*-mediated PC(16:0, 18:2) generation can inhibit ER stress in Th17 and iTreg cells, thus shedding insight into the metabolic control of T cell immunity. Many lipid biosynthesis enzymes are located in the ER membrane, and LPCAT family members are also ER membrane proteins (13, 46). Future studies will clarify whether a specific sub-cellular organelle is associated with *Lpcat4*-mediated PC(16:0, 18:2) generation. In addition, the detailed mechanism for PC-mediated modulation of ER stress, as well as the *in vivo* role of PC(16:0, 18:2) in controlling autoimmunity await future analyses.

In summary, we show that *Setd2*-mediated H3K36me3 is necessary for maintaining the balance of Th17/Treg cell differentiation to restrain autoimmunity. This process is dependent on *Lpcat4*-mediated phosphatidylcholine generation. Our research

adds to our knowledge of the cross-talk between epigenetics and the phospholipid remodeling pathway and identifies *Setd2* as a potential biomarker and therapeutic target for autoimmune disorders.

## Materials and Methods

**Mice.** C57BL/6J (6 to 8 wk of age) mice were obtained from Joint Ventures Sipper BK Experimental Animal Company (Shanghai, China). *Rag2*<sup>-/-</sup> (B6(Cg)-*Rag2*<sup>tm1.1Cgn</sup>/J, 008449) and CD4-cre (STOCK Tg(Cd4-cre)1Cwi/BfluJ) mice were obtained from the Jackson Laboratory. *Setd2*<sup>fl/fl</sup> mice were prepared as described previously (24). All animal experiments conformed to the NIH Guide for the Care and Use of Laboratory Animals, with the approval of the Scientific Investigation Board of Naval Medical University, Shanghai.

Detailed materials and methods are presented fully in *SI Appendix, Materials and Methods*.

**Statistical Analysis.** Statistical analysis was performed using software GraphPad Prism 8.3.0. The data were assessed using the unpaired two-tailed Student's *t* test; *P* values  $\leq 0.05$  were considered statistically significant (\**P* < 0.05, \*\**P* < 0.01, \*\*\**P* < 0.001, \*\*\*\**P* < 0.0001).

**Data, Materials, and Software Availability.** The RNA sequencing data are deposited in the NCBI GEO under accession code [GSE235827](https://www.ncbi.nlm.nih.gov/geo/query/acc.cgi?acc=GSE235827) (27). All other data are included in the manuscript and/or *SI Appendix*.

**ACKNOWLEDGMENTS.** We thank Ms. Nayi Weng and Ms. Yiran Wang (Naval Medical University, Shanghai, China) for their technical assistance. This work was supported by Grants from the National Key R&D Program (2018YFA0507400), National Natural Science Foundation of China (82388201, 32370963, 31870909, and 32070903) and CAMS Innovation Fund for Medical Sciences (2021-I2M-1-017) and China Postdoctoral Science Foundation (2023M740318).

Author affiliations: <sup>a</sup>Department of Immunology, Center for Immunotherapy, Institute of Basic Medical Sciences, Peking Union Medical College, Chinese Academy of Medical Sciences, Beijing 100005, China; <sup>b</sup>National Key Laboratory of Immunology and Inflammation, Institute of Immunology, Naval Medical University, Shanghai 200433, China; <sup>c</sup>Translational Medical Center for Stem Cell Therapy, Shanghai East Hospital, School of Life Sciences and Technology, Tongji University, Shanghai 200120, China; and <sup>d</sup>Institute of Immunology, College of Life Sciences, Nankai University, Tianjin 300071, China

1. A. N. Theofilopoulos, D. H. Kono, R. Baccala, The multiple pathways to autoimmunity. *Nat. Immunol.* **18**, 716–724 (2017).
2. J. Liu, X. Cao, RBP-RNA interactions in the control of autoimmunity and autoinflammation. *Cell Res.* **33**, 97–115 (2023).
3. M. Charabati, M. A. Wheeler, H. L. Weiner, F. J. Quintana, Multiple sclerosis: Neuroimmune crosstalk and therapeutic targeting. *Cell* **186**, 1309–1327 (2023).
4. B. L. Heckmann *et al.*, LC3-associated endocytosis facilitates  $\beta$ -amyloid clearance and mitigates neurodegeneration in murine Alzheimer's disease. *Cell* **178**, 536–551 (2019).
5. N. M. Chapman, M. R. Boothby, H. Chi, Metabolic coordination of T cell quiescence and activation. *Nat. Rev. Immunol.* **20**, 55–70 (2020).
6. D. A. Chisom, A. S. Weinmann, Connections between metabolism and epigenetics in programming cellular differentiation. *Annu. Rev. Immunol.* **36**, 221–246 (2018).
7. D. R. Green, L. Galluzzi, G. Kroemer, Cell biology. Metabolic control of cell death. *Science* **345**, 1250256 (2014).
8. S. A. Lim, W. A.-O. Su, N. M. Chapman, H. Chi, Lipid metabolism in T cell signaling and function. *Nat. Chem. Biol.* **18**, 470–481 (2022).
9. C. H. Patel, R. D. Leone, M. R. Horton, J. D. Powell, Targeting metabolism to regulate immune responses in autoimmunity and cancer. *Nat. Rev. Drug. Discov.* **18**, 669–688 (2019).
10. A. Wagner *et al.*, Metabolic modeling of single Th17 cells reveals regulators of autoimmunity. *Cell* **184**, 4168–4185 (2021).
11. C. Guo *et al.*, SLC38A2 and glutamine signalling in cDC1s dictate anti-tumour immunity. *Nature* **620**, 200–208 (2023), [10.1038/s41586-023-06299-8](https://doi.org/10.1038/s41586-023-06299-8).
12. W. Zou, D. R. Green, Beggars banquet: Metabolism in the tumor immune microenvironment and cancer therapy. *Cell Metab.* **35**, 1101–1113 (2023).
13. B. Wang, P. Tontonoz, Phospholipid remodeling in physiology and disease. *Annu. Rev. Physiol.* **81**, 165–188 (2019).
14. B. Wang *et al.*, Intestinal phospholipid remodeling is required for dietary-lipid uptake and survival on a high-fat diet. *Cell Metab.* **23**, 492–504 (2016).
15. X. Rong *et al.*, ER phospholipid composition modulates lipogenesis during feeding and in obesity. *J. Clin. Invest.* **127**, 3640–3651 (2017).
16. Q. Zhang, X. Cao, Epigenetic regulation of the innate immune response to infection. *Nat. Rev. Immunol.* **19**, 417–432 (2019).
17. Q. Zhang, X. Cao, Epigenetic remodeling in innate immunity and inflammation. *Annu. Rev. Immunol.* **39**, 279–311 (2021).
18. X. Cao, Self-regulation and cross-regulation of pattern-recognition receptor signalling in health and disease. *Nat. Rev. Immunol.* **16**, 35–50 (2016).
19. A. N. Henning, R. Roychoudhuri, N. P. Restifo, Epigenetic control of CD8(+) T cell differentiation. *Nat. Rev. Immunol.* **18**, 340–356 (2018).
20. J. R. Giles *et al.*, Human epigenetic and transcriptional T cell differentiation atlas for identifying functional T cell-specific enhancers. *Immunity* **55**, 557–574 (2022).
21. G. Cavalli, E. Heard, Advances in epigenetics link genetics to the environment and disease. *Nature* **571**, 489–499 (2019).
22. A. T. Phan, A. W. Goldrath, C. K. Glass, Metabolic and epigenetic coordination of T cell and macrophage immunity. *Immunity* **46**, 714–729 (2017).
23. E. J. Wagner, P. B. Carpenter, Understanding the language of Lys36 methylation at histone H3. *Nat. Rev. Mol. Cell Biol.* **13**, 115–126 (2012).
24. K. Chen *et al.*, Methyltransferase SETD2-mediated methylation of STAT1 is critical for interferon antiviral activity. *Cell* **170**, 492–506.e414 (2017).
25. H. Huang *et al.*, Histone H3 trimethylation at lysine 36 guides m(6A) RNA modification co-transcriptionally. *Nature* **567**, 414–419 (2019).
26. M. Liu *et al.*, The histone methyltransferase SETD2 modulates oxidative stress to attenuate experimental colitis. *Redox Biol.* **43**, 102004 (2021).
27. Y. Chen, X. Cao, Data from "Methyltransferase *Setd2* prevents T cell-mediated autoimmune diseases via phospholipid remodeling". NCBI GEO. <https://www.ncbi.nlm.nih.gov/geo/query/acc.cgi?acc=gse235827>. Deposited 26 June 2023.
28. S. Osman, P. Cramer, Structural biology of RNA polymerase II transcription: 20 years on. *Annu. Rev. Cell Dev. Biol.* **36**, 1–34 (2020).
29. K. Chambers, W. J. Judson, A unique lysophospholipid acyltransferase (LPAT) antagonist, CI-976, affects secretory and endocytic membrane trafficking pathways. *J. Cell Sci.* **118**, 3061–3071 (2005).
30. T. Harayama *et al.*, Lysophospholipid acyltransferases mediate phosphatidylcholine diversification to achieve the physical properties required *in vivo*. *Cell Metab.* **20**, 295–305 (2014).
31. X. Rong *et al.*, LXRs regulate ER stress and inflammation through dynamic modulation of membrane phospholipid composition. *Cell Metab.* **18**, 685–697 (2013).

32. C. M. Osowski, F. Urano, Measuring ER stress and the unfolded protein response using mammalian tissue culture system. *Methods Enzymol.* **490**, 71–92 (2011).
33. G. Hotamisligil, R. Davis, Cell signaling and stress responses. *Cold Spring Harb. Perspect. Biol.* **8**, a006072 (2016).
34. J. Yang, X. Yang, H. Zou, M. Li, Oxidative stress and Treg and Th17 dysfunction in systemic lupus erythematosus. *Oxid Med. Cell Longev.* **2016**, 2526174 (2016).
35. K. Atarashi *et al.*, Th17 cell induction by adhesion of microbes to intestinal epithelial cells. *Cell* **163**, 367–380 (2015).
36. P. J. Vernon, D. Tang, Eat-me: Autophagy, phagocytosis, and reactive oxygen species signaling. *Antioxid Redox Signal.* **18**, 677–691 (2013).
37. L. Galluzzi, D. R. Green, Autophagy-independent functions of the autophagy machinery. *Cell* **177**, 1682–1699 (2019).
38. J. Moretti *et al.*, STING senses microbial viability to orchestrate stress-mediated autophagy of the endoplasmic reticulum. *Cell* **171**, 809–823 (2017).
39. E. V. Dang *et al.*, Control of T(H)17/T(reg) balance by hypoxia-inducible factor 1. *Cell* **146**, 772–784 (2011).
40. W. G. Kaelin Jr., P. J. Ratcliffe, Oxygen sensing by metazoans: The central role of the HIF hydroxylase pathway. *Mol. Cell.* **30**, 393–402 (2008).
41. J. Chang *et al.*, Setd2 determines distinct properties of intestinal ILC3 subsets to regulate intestinal immunity. *Cell Rep.* **38**, 110530 (2022).
42. M. P. Wymann, R. Schneiter, Lipid signalling in disease. *Nat. Rev. Mol. Cell Biol.* **9**, 162–176 (2008).
43. Y.A.-O. Endo *et al.*, 1-Oleoyl-lysophosphatidylethanolamine stimulates ROR $\gamma$ t activity in T(H)17 cells. *Sci. Immunol.* **8**, eadd4346 (2023).
44. A. K. Cotte *et al.*, Lysophosphatidylcholine acyltransferase 2-mediated lipid droplet production supports colorectal cancer chemoresistance. *Nat. Commun.* **9**, 322 (2018).
45. M. J. Wolfgang, Remodeling glycerophospholipids affects obesity-related insulin signaling in skeletal muscle. *J. Clin. Invest.* **131**, e148176 (2021).
46. T. Nishimura, C. J. Stefan, Specialized ER membrane domains for lipid metabolism and transport. *Biochim. Biophys. Acta Mol. Cell Biol. Lipids* **1865**, 158492 (2020).